Chemistry & Biology, Vol. 11, 1455–1463, October, 2004, ©2004 Elsevier Ltd. All rights reserved. DOI 10.1016/j.chembiol.2004.08.015

A New Curcumin Derivative, HBC, Interferes with the Cell Cycle Progression of Colon Cancer Cells via Antagonization of the Ca^{2+}/Calmodulin Function

Joong Sup Shim,[1] Jiyong Lee,[1] Hyun-Ju Park,[2] So-Jung Park,[2] and Ho Jeong Kwon[1,*]
[1]Chemical Genomics National Research Laboratory
Department of Bioscience and Biotechnology
Institute of Bioscience
Sejong University
Seoul 143-747
Korea
[2]College of Pharmacy
Sungkyunkwan University
Suwon, Kyungkido 440-746
Korea

Summary

HBC (4-{3,5-Bis-[2-(4-hydroxy-3-methoxy-phenyl)-ethyl]-4,5-dihydro-pyrazol-1-yl}-benzoic acid) is a recently developed curcumin derivative which exhibits potent inhibitory activities against the proliferation of several tumor cell lines. In the present study, we identified Ca^{2+}/calmodulin (Ca^{2+}/CaM) as a direct target protein of HBC using phage display biopanning. Ca^{2+}/CaM-expressing phages specifically bound to the immobilized HBC, and the binding was Ca^{2+} dependent. Moreover, flexible docking modeling demonstrated that HBC is compatible with the binding cavity for a known inhibitor, W7, in the C-terminal hydrophobic pocket of Ca^{2+}/CaM. In biological systems, HBC induced prolonged phosphorylation of ERK1/2 and activated $p21^{WAF1}$ expression, resulting in the induction of G_0/G_1 cell cycle arrest in HCT15 colon cancer cells. These results suggest that HBC inhibits the cell cycle progression of colon cancer cells via antagonizing of Ca^{2+}/CaM functions.

Introduction

Recent use of chemical genetics approaches makes possible the mining and the identification of specific target proteins of biologically active chemicals [1]. Affinity matrix-based protein purification [2] and phage display biopanning [3] have been developed as key solutions for this aim. These methods are based on the affinity selection of target proteins by immobilized bioactive chemicals. Such approaches have been successfully employed to identify the specific target of a number of bioactive chemicals, including FK506 [2], rapamycin [4], trapoxin [5], radicicol [6], fumagillin [7], and taxol [8]. Recently, a large number of chemicals that are biologically interesting but with largely unknown mechanism have been isolated from natural products and chemical libraries. Identification of targets of such chemicals can provide tremendous benefits in functional genomics and disease-related new drug development.

We previously developed several novel curcumin derivatives and evaluated their biological activities [9]. Among them, 4-{3,5-bis-[2-(4-hydroxy-3-methoxy-phenyl)-ethyl]-4,5-dihydro-pyrazol-1-yl}-benzoic acid (referred to as HBC) showed potent inhibitory activities against the proliferation of several human cancer cells. However, the mechanisms underlying how HBC inhibits tumor cell growth are entirely unknown. Interestingly, it turned out that HBC did not inhibit the activity of CD13/aminopeptidase N (APN), one of the direct binding targets of curcumin [10]. It has been speculated that HBC may target a new protein critical for cell growth, rather than APN, in tumor cells. We thus attempted to isolate the target protein of HBC using chemical genetics approaches. The affinity matrix-based protein purification method requires high affinity of chemicals to their target proteins [11]. However, HBC, which exhibits biological activity around the 10 μM range, is likely to have relatively low affinity to its putative target protein, making it unsuitable for affinity matrix-based protein purification. Therefore, we conducted phage display biopanning, which is widely used for target identification of low affinity ligands because the method can isolate proteins existing at extremely low amounts in cells [3]. Using bioactive biotinyl-HBC and phage display biopanning analysis, we presently isolated Ca^{2+}/calmodulin (Ca^{2+}/CaM) as a direct target protein of HBC.

Ca^{2+}/CaM is a calcium binding protein which is implicated in a variety of cellular functions, including cell growth and proliferation [12–14]. Ca^{2+}/CaM itself does not show any catalytic activity but regulates activities of a number of Ca^{2+}/CaM-dependent enzymes, such as myosin light chain kinase (MLCK) [15], CaM-kinases [16], phosphodiesterase [17], protein phosphatase [18], and nitric oxide synthase [19]. Recently, evidence has shown that Ca^{2+}/CaM is implicated in cancers; e.g., an abnormal expression of Ca^{2+}/CaM often occurs in certain tumors [20], and specific antagonists of Ca^{2+}/CaM inhibit the growth of a variety of tumor cells [21–23]. Thus, Ca^{2+}/CaM has been recognized as a potential target for cancer chemotherapy [24, 25]. The present study shows for the first time that HBC is a new antagonist of Ca^{2+}/CaM and provides a critical clue for deciphering molecular mechanisms underlying the inhibition of tumor cell proliferation by HBC. The identification and validation of Ca^{2+}/CaM as a functional target of HBC are described.

Results

Antiproliferative Activity of HBC on Tumor Cells

Ongoing studies have focused on the identification of new target proteins that play a critical role in cellular proliferation. HBC has been developed recently as a new curcumin derivative that inhibits the proliferation of several tumor cell lines. Thus, we selected HBC as a chemical genetics probe for the identification of such proteins. In the first step of the study, we investigated the inhibitory activity of HBC on the proliferation of HCT15 colon carcinoma cells, which showed the most

*Correspondence: kwonhj@sejong.ac.kr

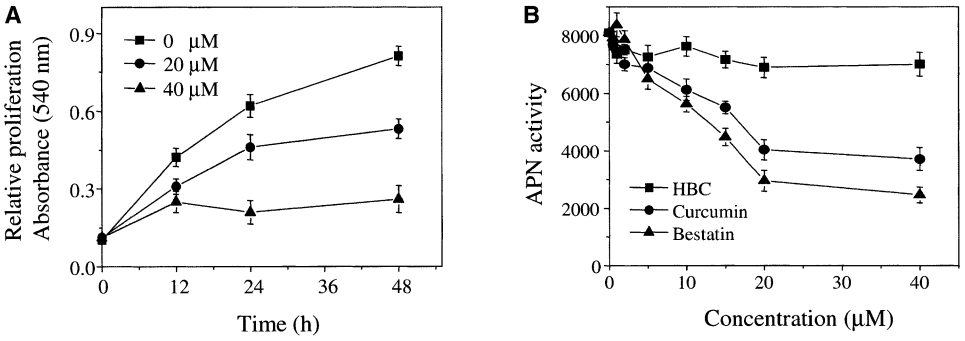

Figure 1. Effect of HBC on the Proliferation of HCT15 Cells

(A) Time- and dose-responses of HBC on HCT15 cell proliferation are shown. The cell proliferation was measured by an MTT assay.
(B) Effect of HBC on the activity of APN. The assay procedure was described previously [10]. Curcumin and bestatin were used as positive control compounds. All data represent mean ± SE from three independent experiments.

sensitive response against the HBC treatment (data not shown). HBC dose- and time-dependently inhibited the proliferation of HCT15 cells with an IC_{50} of 20 μM (Figure 1A). The proliferation of HCT15 cells was completely inhibited by 40 μM treatment with HBC. It was not cytotoxic, because the population of HBC-treated cells at the end of the assay was no less than the initial cell population. We previously demonstrated that hydrazinocurcumin, a novel curcumin derivative, does not inhibit aminopeptidase N activity [10]. In the present study, HBC was also examined for effect on APN activity. The result shown in Figure 1B demonstrates that, like hydrazinocurcumin, HBC does not inhibit APN activity at any concentration used in this study. Therefore, we speculated that there is a different cellular target of HBC rather than APN in mammalian cells that is critical for cell growth.

Identification of Ca^{2+}/CaM as a Cellular Binding Partner for HBC

To isolate the direct binding protein of HBC, we first synthesized biotinyl-HBC as a molecular probe for target identification (Figure 2A). The biological activity of the biotinyl-HBC was assessed via its inhibitory activity against the proliferation of HCT15 cells. Biotinyl-HBC inhibited the proliferation of the colon cancer cells with an IC_{50} of 42 μM, which is 2-fold less potent than that of the parental compound, HBC, but still indicates biological activity (Figure 2B). Biotinyl-HBC was then immobilized onto streptavidin-coated wells, and T7 phages encoding human cDNA libraries were used for affinity selection of HBC binding protein. Increased phage particles were bound to HBC in proportion to each round of biopanning, implying that specific HBC binding phages were enriched after progression of biopanning rounds (Figure 2C). After the fourth round of biopanning, phage particles that specifically bound to HBC were isolated using a plaque forming assay and then analyzed for DNA sequencing as described in the Experimental Procedures. A total of 17 phage plaques were isolated for sequence analysis, and the resulting data were then subjected to sequence homology analysis using the BLAST search on the web (www.ncbi.nlm.nih.gov/BLAST). Among 17 phage plaques isolated, 12 were identified as CaM-coding phages (about 70% of total isolated phage clones). The translated sequence analysis demonstrated that the coding sequences of the CaM-phages are 100% identical to C-terminal fragment (86 to ~149 aa) of human CaM (Figure 2D). The other five phage clones were identified as cytochrome b, farnesyltransferase, and three different unknown genes, and were subsequently revealed as nonspecific binders through phage binding assays (data not shown).

Ca^{2+} Is Essentially Required for the Binding of HBC to CaM

We next investigated the binding specificity of HBC to CaM-expressing phage (CaM-phage) using control biotin and nonspecific phage encoding cytochrome b gene (Cyt. b-phage). As a result, CaM-phage specifically bound to the biotinyl-HBC, but not to control biotin immobilized on streptavidin (Figure 3A). Moreover, CaM-phage, but not Cyt. b-phage, was able to bind to the biotinyl-HBC immobilized on streptavidin. These data indicate that CaM is a specific binding protein of HBC. CaM is a major cellular Ca^{2+} binding protein in which conformational changes occur after the binding of Ca^{2+} to its EF-hand motifs [26]. These conformational changes of Ca^{2+}/CaM allow interaction with several Ca^{2+}/CaM target proteins and its antagonists [27]. Thus, we investigated whether Ca^{2+} is required for the binding of CaM to immobilized HBC. In the absence of exogenous Ca^{2+}, CaM-phage can bind to immobilized HBC with high affinity (Figure 3B), and exogenously added Ca^{2+} slightly increased the binding of CaM-phage to immobilized HBC. However, the addition of a Ca^{2+} chelator, ethylene glycol-bis(β-aminoethylether)-tetraacetic acid (EGTA), completely inhibited the binding of CaM-phage to immobilized HBC (Figure 3C). To exclude the possibility that EGTA itself inhibits the binding between HBC and CaM, the experiment was performed in the presence of EGTA and an excess amount of Ca^{2+}. As shown in Figure 3D, an excess amount of Ca^{2+} (10 mM) fully reverses EGTA (2 mM)-induced disruption of the binding between HBC and CaM. These results demonstrate that Ca^{2+} is essentially required for the binding between HBC and CaM and suggest that CaM expressed in the T7 phage may be a Ca^{2+} bound form.

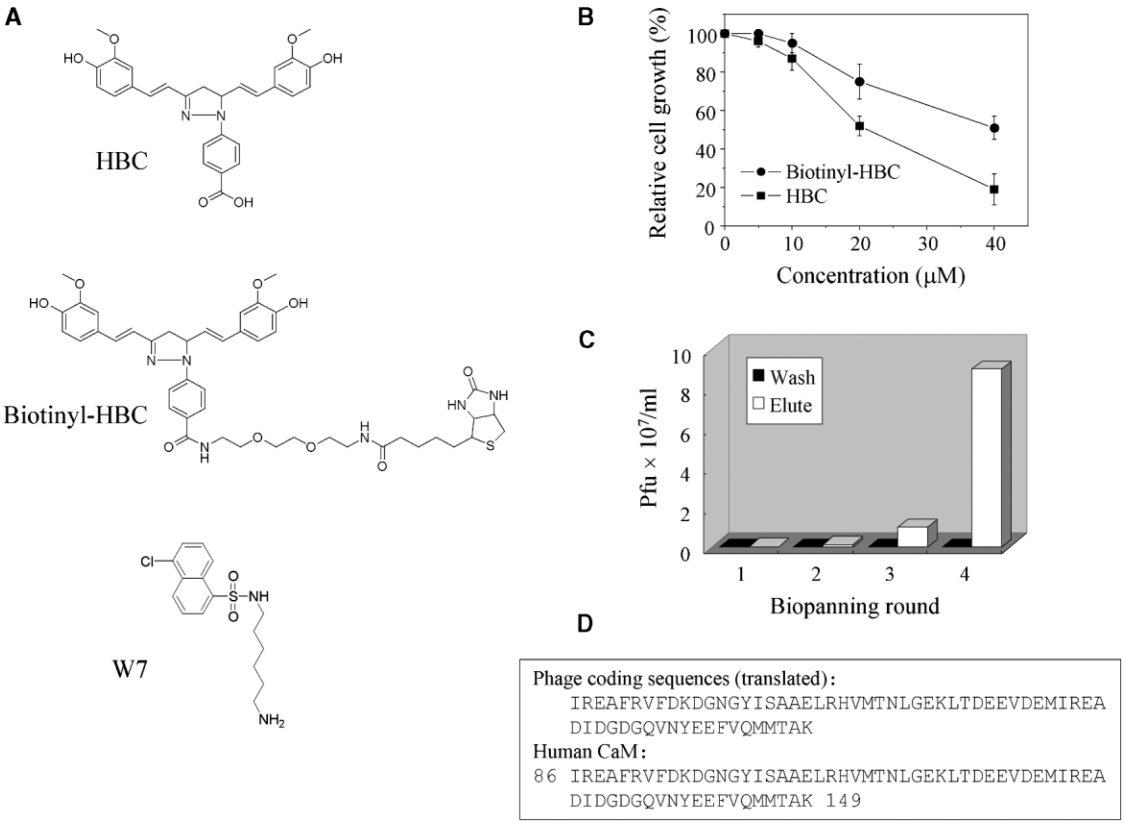

Figure 2. Identification of HBC Binding Protein Using Phage Display Biopanning

(A) The structures of HBC, its molecular probe (biotinyl-HBC), and W7 are shown.

(B) Effects of HBC and biotinyl-HBC on the proliferation of HCT15 cells. The cells were treated with each compound for 72 hr, and an MTT assay was performed to evaluate the biological activity of the compounds.

(C) Analysis of HBC binding phage particles eluted after each round of biopanning. "Wash" indicates nonspecific phages bound to biotinyl-HBC immobilized on a streptavidin-coated well.

(D) Sequence homology between human CaM and the coding protein of HBC binding phage. The phage sequences were 100% identical to the C-terminal (86–149) of human CaM.

Biochemical and Biophysical Validation of the Interaction between HBC and Ca^{2+}/CaM

Three-dimensional structures of Ca^{2+}/CaM revealed that Ca^{2+}/CaM has two hydrophobic pockets on the surface of each N- and C-terminal domain [28]. These hydrophobic pockets are essential for Ca^{2+}/CaM to bind target enzymes, peptides, and antagonists. Extensive studies have shown that Ca^{2+}/CaM antagonists N-(6-amino-

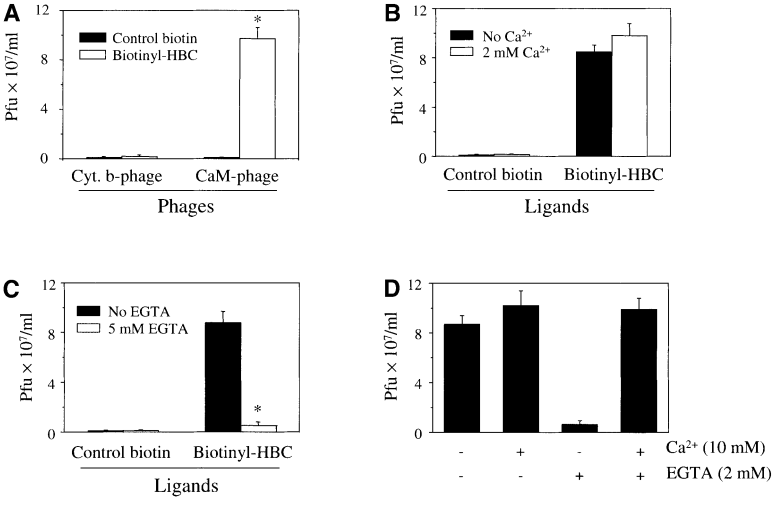

Figure 3. Effect of Ca^{2+} and EGTA on the Binding of HBC to Ca^{2+}/CaM

(A) The specificity of interaction between HBC and CaM-expressing phage. Control biotin and Cyt. b-phage were used as negative controls for biotinyl-HBC and CaM-phage, respectively. *$p < 0.0001$ versus Cyt. b-phage.

(B) The effect of Ca^{2+} on the binding of CaM-phage to immobilized HBC is shown.

(C) The effect of EGTA on the binding of CaM-phage to immobilized HBC is shown. *$p < 0.0002$ versus no EGTA control.

(D) Effect of an excess amount of Ca^{2+} on EGTA-induced disruption of the binding between HBC and CaM-phage. All data represent mean ± SE from three independent experiments.

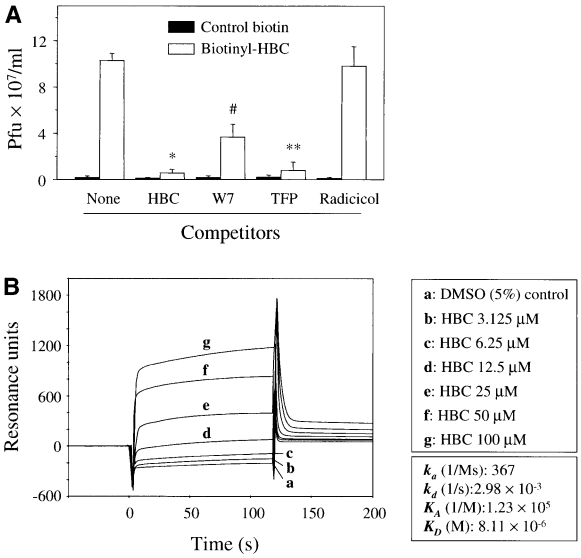

Figure 4. Biochemical and Biophysical Analyses of the Binding between HBC and Ca^{2+}/CaM

(A) Effects of several competitors on the binding of CaM C-phage to immobilized HBC. Control biotin was used as a negative control in each competitor. All competitors were used at a concentration of 50 μM. *p < 0.0001, #p < 0.001, and **p < 0.0004 versus no competitor control. Data represent mean ± SE from three independent experiments.

(B) BIAcore analysis of interaction between HBC and Ca^{2+}/CaM. Purified Ca^{2+}/CaM was immobilized on a CM5 sensor chip, and various concentrations of HBC were loaded into the sensor cell. Binding sensorgrams were obtained from the BIAcore evaluation software. Kinetic parameters of k_a, k_d, K_A, and K_D are shown.

hexyl)-5-chloro-1-naphthalensulfonamide (W7) and trifluoperazine (TFP) can bind to each hydrophobic pocket of N- and C-terminal domains of CaM in a Ca^{2+}-dependent manner and may inhibit the access of CaM-dependent target enzymes [29, 30]. We next investigated whether the interaction between HBC and Ca^{2+}/CaM is influenced by several competitors, using phage display binding analyses. A large molar excess of free HBC completely blocked the binding of CaM-phage to immobilized HBC (Figure 4A). W7 and TFP also significantly inhibited the interaction between HBC and CaM-phage. The results from the competition assay suggest that HBC has the highest binding affinity to CaM-phage among three Ca^{2+}/CaM antagonists. However, another cell cycle inhibitor, radicicol [31], did not interfere with the interaction between two molecules. These data suggest that HBC and two Ca^{2+}/CaM antagonists share a common binding site within Ca^{2+}/CaM. We next examined the real-time interaction between HBC and intact Ca^{2+}/CaM using surface plasmon resonance (BIAcore) analysis. Purified bovine brain CaM was immobilized on a surface of a BIAcore sensor chip, and various concentrations of HBC were injected into the sensor cells to monitor the interaction between two molecules. Strong binding curves of HBC were observed in the sensorgrams of BIAcore (Figure 4B). The kinetic parameters of k_a, k_d, and K_D were determined using BIAcore evaluation software. As shown in Figure 4B, the apparent dissociation constant (K_D) of HBC binding to Ca^{2+}/CaM was calculated as 8.11×10^{-6} M. These results clearly demonstrate that Ca^{2+}/CaM is a direct binding protein of HBC.

Analysis of the Docking Model of HBC Bound to C-Terminal Ca^{2+}/CaM Domain

A previous NMR structural study revealed that W7 binds into the hydrophobic pocket of the C/N-terminal domain of Ca^{2+} bound CaM, which is the essential binding site for target enzymes [30]. This study also suggested that van der Waals interactions between the 5-chloro-naphthalene ring of W7 and aromatic/aliphatic amino acid residues in the active site are crucial for competitive inhibition of CaM-mediated enzyme activation. To examine a possible binding mode of HBC in the hydrophobic pocket of Ca^{2+}/CaM, a flexible docking study was conducted using the FlexX program. The reference protein coordinate used for docking was taken from the solution structure of the C-terminal domain of Ca^{2+}/CaM in complex with W7 (PDB entry: 1MUX) [30]. Both S- and R-form structures of HBC were prepared and then docked into the W7 bound pocket. As shown in Figure 5A, docking results showed that R-HBC is not compatible with the W7 binding cavity of Ca^{2+}/CaM, suggesting that R-HBC may not be an active form, while S-HBC nicely fit into the hydrophobic pocket. The FlexX-docked pose of S-HBC is demonstrated in contrast to the NMR-derived binding pose of W7 in Figure 5B. One vinylguaiacol arm of S-HBC anchors deep into the same pocket as is occupied by the chloronaphthalene ring of W7, and the phenolic hydroxy group forms a hydrogen bond with backbone amide of Met124. The remaining vinylguaiacol arm and benzoic acid-linked hydrazine moiety of S-HBC cap the surface of protein. Especially, benzoic acid-linked hydrazine group is fully superimposed over the *N*-aminohexyl sulfonamido side chain of W7 on the surface of protein. Conclusively, the binding mode of S-HBC generated by FlexX revealed that the structure of the molecule is a good fit into the W7 binding cavity of Ca^{2+}/CaM, in which one vinylguaiacol arm and the benzoic acid-linked hydrazine moiety play a role as a capping group bigger than that of W7 and one vinylguaiacol group forms hydrophobic interaction with amino residues in the active site pocket. The present modeling study well elucidates the experimental result showing that HBC has CaM binding capacity comparable to W7.

HBC Induces Sustained Phosphorylation of ERK1/2

We finally investigated the biological significance of the binding of HBC to Ca^{2+}/CaM and attempted to validate Ca^{2+}/CaM as a target protein of the compound for its biological activity. Recent reports showed that extracellular signal-regulated kinase (ERK) 1/2 is a critical mediator of Ca^{2+}/CaM signaling [32–34]. Several antagonists of Ca^{2+}/CaM induced sustained phosphorylation of ERK1/2 and inhibited tumor cell proliferation. Thus, we investigated the phosphorylation status of ERK1/2 in tumor cells treated with HBC. Among eight cell lines tested in this study, HCT15 turned out to express a relatively high level of Ca^{2+}/CaM compared to others and was selected as a model cell line for further study (data not shown). In serum-starved HCT15 cells, HBC time dependently induced ERK1/2 phosphorylation (Fig-

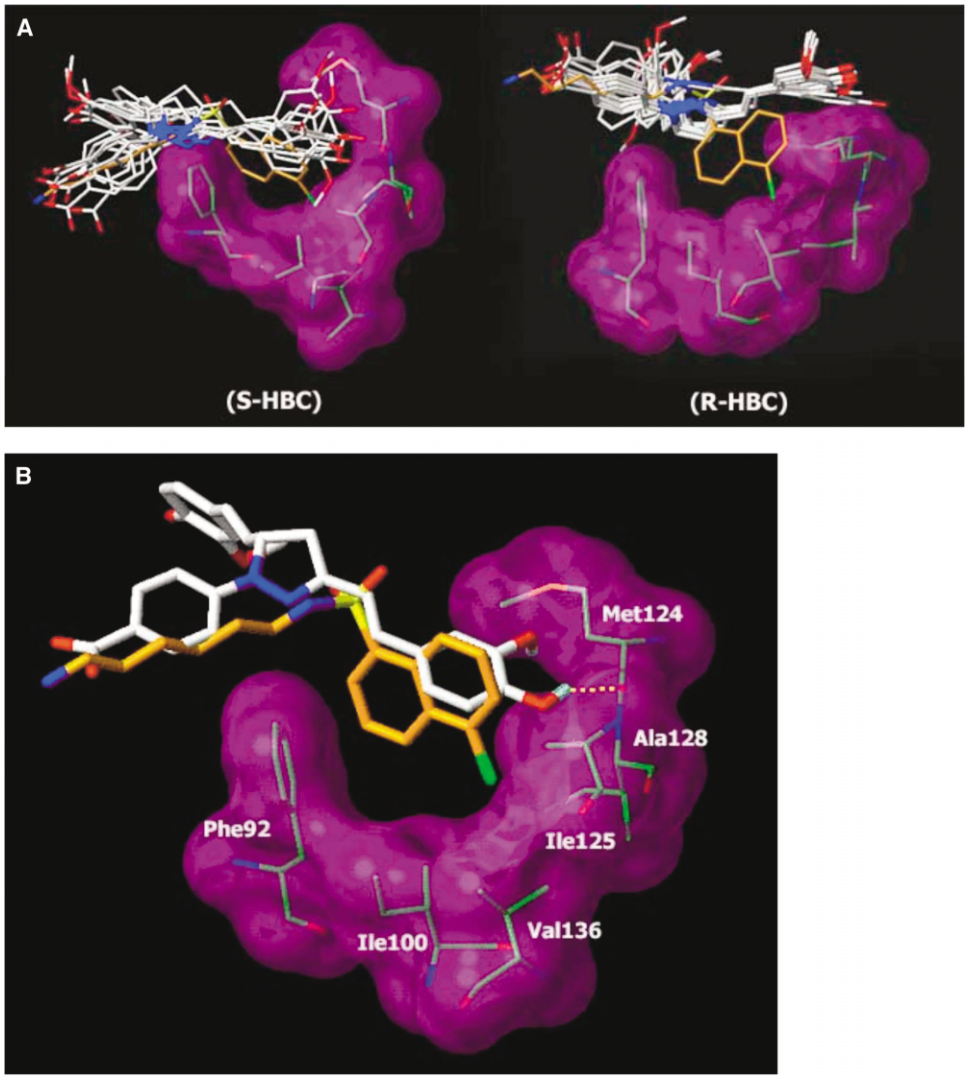

Figure 5. Docking Model of HBC in Complex with the C-Terminal Ca^{2+}/CaM Domain

(A) FlexX-docked conformational ensemble of S-HBC versus R-HBC superimposed onto the NMR-structure of W7 (orange carbon) bound to the C-terminal Ca^{2+}/CaM domain.

(B) The docking mode of the top-ranked conformer of S-HBC (gray carbon) obtained from FlexX. The Connolly molecular surface of the active site is shown in purple, with the amino acid residues occupying the active site. Hydrogen atoms are not shown for clarity. The yellow dotted line indicates hydrogen bonding interaction (d = 1.244 Å).

ure 6, upper panel). The phosphorylation of ERK1/2 was retained up to 12 hr after treatment with HBC in serum-starved HCT15 cells. The right panels in Figure 6 show the quantitative data for the phosphorylation pattern of ERK1/2, which provides ratios of phosphorylated to unphosphorylated ERK1/2. A high concentration of serum (10%) also activated the phosphorylation of ERK1/2, but the activation was transient (Figure 6, middle panel). In contrast, HBC treatment caused sustained phosphorylation of ERK1/2 in HCT15 cells in the presence of 10% serum (Figure 6, lower panel). These data demonstrate that HBC binds to Ca^{2+}/CaM and influences the downstream signaling pathways of Ca^{2+}/CaM in the cells.

HBC Inhibits Cell Cycle Progression of HCT15 Cells by Inducing G_0/G_1 Arrest

Accumulating evidence has shown that several antagonists of Ca^{2+}/CaM activate $p21^{WAF1}$ expression and subsequently inhibit cell cycle progression of tumor cells via induction of G_0/G_1 cell cycle arrest [32, 33, 35]. We thus examined the effect of HBC on $p21^{WAF1}$ accumulation in HCT15 cells. Western blot analysis revealed that HBC dose- and time dependently increased the level of $p21^{WAF1}$ expression (Figures 7A and 7B). W7 also activated $p21^{WAF1}$ expression in HCT15 cells in a similar pattern as that of HBC (Figure 7B). We next investigated whether HBC inhibits the tumor cell proliferation by causing arrest in a specific phase of the cell cycle. HCT15 cells were synchronized by serum deprivation for 24 hr, and then we added serum, allowing them to reinitiate the cell cycle. The cell cycle distribution of HCT15 cells was analyzed by flow cytometry. HBC dose dependently inhibited cell cycle progression of HCT15 cells (Figure 7C, upper panels). Accumulation of cells in G_1 phase and the reduction in S phase demonstrated that HBC induced G_0/G_1 cell cycle arrest. The time

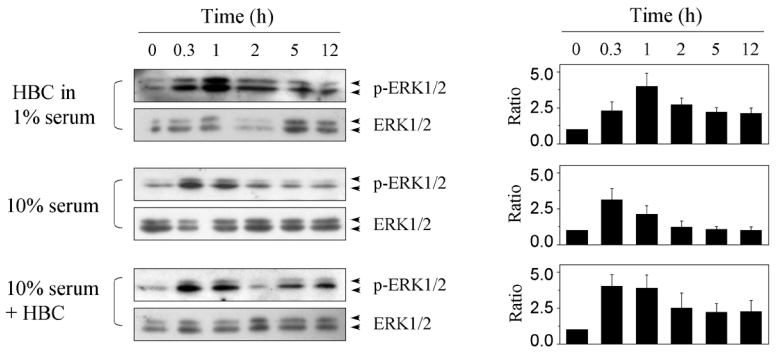

Figure 6. Analysis of ERK1/2 Phosphorylation in HCT15 Cells

Effects of HBC on the phosphorylation of ERK1/2. (Upper panel) HCT15 cells were starved in 1% FBS for 24 hr, and HBC was treated for the indicated time points. Anti-phospho-ERK1/2 antibody was used to detect ERK1/2 phosphorylation. The levels of ERK1/2 and tubulin were used as internal controls. (Middle and lower panels) Effect of 10% serum only or 10% serum with HBC on the phosphorylation of ERK1/2 is shown. Figures were selected as representative data from three independent experiments. (Right panels) Ratios of phosphorylated to unphosphorylated ERK1/2 were determined by densitometry. The phosphorylation ratio at each 0 hr (basal level phosphorylation) was normalized to 1 and used as a control in each experiment. Data are mean ± SE from at least three independent experiments.

course analysis showed as well the induction of G_0/G_1 cell cycle arrest by HBC (Figure 7C, lower panels). W7 also induced G_0/G_1 cell cycle arrest in HCT15 cells (data not shown). These results clearly demonstrate that the antiproliferative activity of HBC against HCT15 cells happens, at least in part, through the antagonization of the Ca^{2+}/CaM function in colorectal carcinoma cells.

Discussion

Chemical genetics is an emerging research engine to study unidentified protein functions using biologically active small molecules. Several small molecules which are biologically interesting but are largely unknown in their action mechanisms have been attractive targets for chemical genetics studies [2, 4–7]. A large number of such small molecules have been isolated from natural products and chemical libraries so far. Identification of intracellular target proteins of these biologically interesting small molecules will have a tremendous impact on both functional genomics and drug development.

We previously developed HBC as a novel curcumin derivative and investigated its biological activity. The present study focuses on the identification of a putative target protein of HBC in mammalian cells, using a chemical genetics approach. To identify the cellular target protein of HBC, we tried to isolate the direct binding protein of the compound from genomic libraries using phage display biopanning. The results from in vitro and cell-based assays demonstrate that Ca^{2+}/CaM is a putative target protein of HBC.

Ca^{2+}/CaM consists of N- and C-terminal domains which contain two EF-hand Ca^{2+} binding motifs in each domain [26]. The three-dimensional structures of Ca^{2+}/CaM revealed that Ca^{2+} binding to apo-CaM causes conformational changes from the closed to the open form [36, 37]. This conformational change can generate a hydrophobic pocket on the surface of each domain and provides binding sites for Ca^{2+}/CaM target enzymes as well as several antagonists [27–30]. Well-known Ca^{2+}/CaM antagonists TFP and W7 can bind to both N- and C-terminal hydrophobic pockets [29, 30]. In our study, HBC specifically binds to Ca^{2+}/CaM-expressing phages in a Ca^{2+}-dependent manner. Moreover, TFP and W7

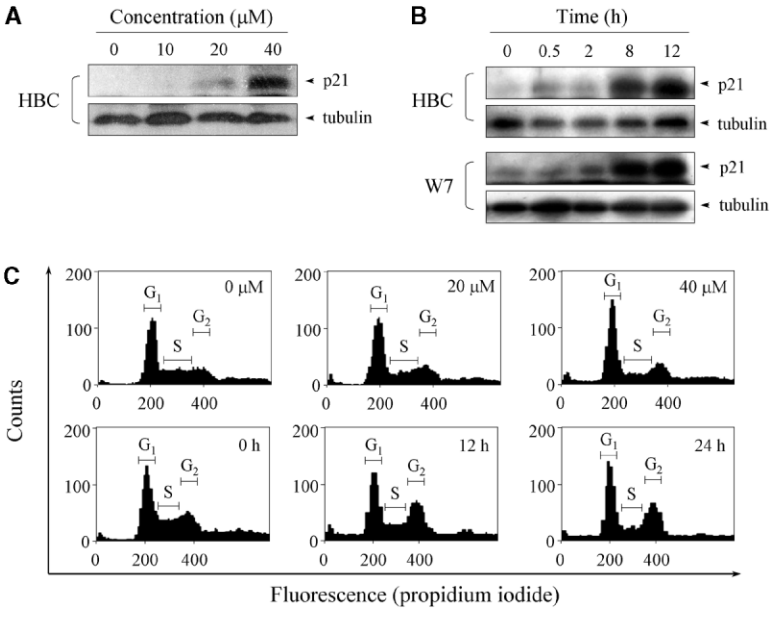

Figure 7. Analyses of $p21^{WAF1}$ Expression and Cell Cycle Progression of HCT15 Cells

(A) Dose response of HBC on the expression of $p21^{WAF1}$. The level of tubulin was used as an internal control for normalization.

(B) Time response of HBC on the expression of $p21^{WAF1}$. W7 was used as a positive control compound.

(C) Dose- (upper panels) and time (lower panels) responses of HBC on the cell cycle distribution of HCT15 cells are shown. Figures were selected as representative data from three independent experiments.

specifically block the binding of HBC to Ca^{2+}/CaM, suggesting that HBC may bind to the hydrophobic pocket of each domain of Ca^{2+}/CaM. Flexible docking analysis of the binding of HBC to the C-terminal hydrophobic pocket of Ca^{2+}/CaM further supported this possibility. In the docking model, S-HBC, but not R-HBC, nicely fits into the W7 binding cavity in the C-terminal hydrophobic pocket of Ca^{2+}/CaM. Three-dimensional structure analysis of the binding between two molecules will help to decipher the exact binding mode of HBC to Ca^{2+}/CaM. The interaction between HBC and full-length Ca^{2+}/CaM was confirmed by surface plasmon resonance analysis. The apparent K_D value of the binding appears at 8.11 μM, which is similar to that of TFP and W-7 (ranging from 1 to 8 μM for TFP and 11 μM for W-7) [38–40]. These data demonstrate that HBC directly binds to Ca^{2+}/CaM with a relatively high affinity.

Ca^{2+}/CaM is a multifunctional protein which binds to a variety of cellular proteins and regulates their activities. Recently, several antagonists of Ca^{2+}/CaM were reported to activate ERK1/2 and then regulate downstream target gene expression [32–34]. They include $p21^{WAF1}$ [32] and Egr-1 [34]. These studies demonstrated that ERK1/2 is a critical mediator for Ca^{2+}/CaM signaling in cell cycle regulation. ERK1/2 is a serine/threonine protein kinase which is rapidly activated by extracellular mitogenic signals and contributes to cellular proliferation [41, 42]. However, sustained phosphorylation of ERK1/2 has been reported to suppress cell cycle progression by the induction of $p21^{WAF1}$ and in turn inhibit cancerous growth of tumor cells [43, 44]. Thus, the strength and duration of ERK1/2 phosphorylation seem to be a critical criteria for its role in the tumor promoting or suppressive function. Our data demonstrate that HBC induces sustained ERK1/2 phosphorylation in HCT15 cells in the presence of both low and high concentrations of serum. Moreover, HBC highly increased the expression of $p21^{WAF1}$ in HCT15 cells and inhibited the cell cycle progression of the cells by inducing G_0/G_1 arrest. These data suggest that HBC inhibits cell cycle progression of the colon cancer cells via ERK1/2/$p21^{WAF1}$ pathways and demonstrate that Ca^{2+}/CaM is a biologically relevant target of HBC in mammalian cells.

Recent strategies for cancer chemotherapy have been focused on the development of new cancer targets that are "single target with multiple effects" [45]. Ca^{2+}/CaM possesses a high potential for being a promising cancer target, because (1) abnormal expression of Ca^{2+}/CaM often occurs in several cancer types [20, 24, 25], and (2) Ca^{2+}/CaM is involved in a number of cellular signaling pathways via regulation of the activities of a variety of its client proteins [12–19]. Development of more potent derivatives of HBC using structure-activity relationship analysis, and in vivo efficacy validation of such compounds, will be our next challenge for new drug development targeting Ca^{2+}/CaM in cancer.

Significance

HBC is a synthetic benzoic acid derivative of curcumin, which shows different biological activities from the parental compound curcumin. We utilized phage display biopanning analysis to identify the cellular target protein of HBC from genome-wide human cDNA libraries. As a result, we isolated a major binding protein of HBC from the phage libraries and subsequently identified Ca^{2+}/CaM as a putative target protein of HBC. Direct interaction between HBC and Ca^{2+}/CaM was confirmed using both phage display binding assay and surface plasmon resonance analysis. Flexible docking modeling of the binding between HBC and Ca^{2+}/CaM suggests a possible binding mode of the new Ca^{2+}/CaM antagonist. In biological systems, HBC induces sustained phosphorylation of ERK1/2 and activates $p21^{WAF1}$ expression, resulting in the suppression of the cell cycle progression of HCT15 colon cancer cells. These biological activities of HBC are similar to those of other Ca^{2+}/CaM antagonists, suggesting that Ca^{2+}/CaM is a biologically relevant target of HBC. The present study demonstrates that HBC is a new Ca^{2+}/CaM antagonist with a unique structure and offers a lead compound for the development of more potent Ca^{2+}/CaM antagonists. Moreover, this study support the idea that Ca^{2+}/CaM is an emerging target for antitumor drug development.

Experimental Procedures

Materials

All docking experiments were performed with Sybyl (version 6.9, Tripos Inc., St. Louis, MO) on an SGI-Octane 2 workstation with a single 475 MHz processor and 128 MB main memory.

Cell Culture and Growth Assay

HCT15 colon carcinoma cells were grown in Dulbecco's modified Eagle's medium (DMEM) supplemented with 10% fetal bovine serum (FBS). The cells were maintained in a humidified incubator supplemented with 5% CO_2. The proliferation of the tumor cells was measured using a 3-(4,5-dimethylthiazol-2-yl)-2,5-diphenyltetrazolium bromide (MTT) assay. Cells were seeded in 96-well plates (5×10^3 cells/well) and incubated for 24 hr. The cells were treated with either HBC or biotinyl-HBC at various concentrations and time conditions. At the end of the assay, MTT (50 μg/ml) was added to each well, and the incubation was continued for 4 hr. MTT-formazan in each well was dissolved in 150 μl DMSO, and the absorbance was read at 540 nm using a microplate reader (Bio-Tek Instrument Inc., Winooski, VT).

Synthesis of Biotinyl-HBC

To a stirred solution of HBC (10 mg, 0.021 mmol) and EZ-Link biotin-PEO-amine (9.4 mg, 0.026 mmol, Pierce Biotechnology Inc., Rockford, IL) in DMF (3 ml) was added EDC (5.0 mg, 0.026 mmol) and HOBt (3.5 mg, 0.026 mmol) at 0°C. The reaction mixture was allowed to warm to room temperature and stirred overnight. Brine (6 ml) was added to the reaction mixture, and the resulting aqueous solution was extracted with EtOAc (5 ml × 3). The combined organic layer was washed with 1 N HCl (4 ml) and brine (4 ml), dried over $MgSO_4$, filtered, and concentrated in vacuo. The crude product was purified by flash column chromatography (CH_2Cl_2:MeOH = 10: 1) to afford pure biotin linked HBC compound in 85% yield. MALDI-MS: calculated (M = 843.0); found $(M-H)^-$ 841.9.

Phage Display Biopanning

Biotinyl-HBC diluted in Tris-buffered saline (TBS [pH 7.5]) was immobilized to a streptavidin-coated well (Pierce Biotechnology, Inc.) at a concentration of 5 μM. T7 phage particles encoding human cDNA libraries from liver tumor, normal liver, Alzheimer's brain, normal brain, and normal stomach tissues (Novagen, Madison, WI) were diluted in TBS (6×10^9 pfu/ml) and added to the HBC-immobilized wells. After incubation for 1 hr at room temperature with gentle shaking, the well plate was washed ten times with TBS, and bound

phage particles were eluted with 100 μM HBC diluted in TBS for 1 hr. The eluted phage particles were amplified after infection into *E. coli* strain BLT5615, and the amplified phage particles were used for second round biopanning. After fourth round biopanning, eluted phages were infected in to BLT5615 grown on an LB agar plate supplemented with 50 μg/ml ampicillin. The plaques formed on the agar plate were isolated, and the DNAs from the isolated plaques were sequenced with the PRISM Dye Terminator Cycle Sequencing Ready Reaction Kit (Applied Biosystems, Foster City, CA).

Surface Plasmon Resonance Analysis

Purified bovine brain CaM (Calbiochem, San Diego, CA) was covalently linked to a CM5 sensor chip with the surface thiol coupling method according to the manufacturer's instructions (BIAcore AB, Uppsala, Sweden). CaM was modified to a thiol-containing protein by incubation with a molar excess of 2-(2-pyridinyldithio)ethaneamine (PDEA), followed by 0.4 M N-ethyl-N′-(3-diethylaminopropyl)-carbodiimide (EDC) in water for 1 hr on ice. Unreacted reagents were removed by an Amicon microconcentrator (Millipore, Bedford, MA). The surface matrix of the CM5 sensor chip was activated by a 2 min injection of an aqueous solution of 0.2 M EDC and 50 mM N-hydroxysuccinimide (NHS), and subsequently by a 3 min injection of 40 mM cystamine dihydrochloride solution. The reduction of surface thiol was achieved by a 3 min injection of 0.1 M dithiothreitol (DTT). Thiol-modified CaM (200 μg/ml) diluted in sodium acetate buffer (pH 4.0) was injected into the sensor cells for 7 min. All coupling reactions were performed at a flow rate of 5 μl/min. Residual cystamine molecules on the surface of the sensor chip were inactivated by injection of 20 mM PDEA-1 M NaCl solution for 4 min. For the binding analysis, compounds in the running buffer (10 mM HEPES [pH 7.4], 150 mM NaCl, and 3 mM EDTA) containing 5% DMSO were injected at a flow rate of 30 μl/min. Association and dissociation curves were obtained on a BIAcore 2000. The surface of the sensor chip was regenerated by injection of 10 μl of the regeneration buffer (10 mM NaCl and 0.1 mM NaOH). The SPR response curves were analyzed with BIAcore Evaluations software, version 3.1. The dissociation rate constant (k_d) was determined from a plot of $\ln(R_0/R)$ versus time, with R being the surface plasmon resonance signal at time t; the association rate constant (k_a) was determined from a plot of $\ln(\mathrm{abs}(dR/dt))$ versus time. The apparent association and dissociation constants were calculated from the kinetic constants; $K_A = k_a/k_d$, $K_D = k_d/k_a$.

Docking Modeling of the HBC:Ca^{2+}/CaM Complex

The structure of the ligand (R/S-HBC) was prepared in MOL2 format using the sketcher module of Sybyl 6.9, and Gasteiger-Huckel charges were assigned to the ligand atoms and then energy-minimized until converged to a maximum derivative of 0.001 kcal mol^{-1} $Å^{-1}$. To obtain a conformational ensemble of HBC, molecular dynamics was run with a simulated annealing protocol. The calculation followed the temperature protocol beginning at 700 K and gradually cooling down to 200 K for 1000 fs and was run for five cycles. The dynamics result was analyzed, and 42 conformers were randomly selected. The selected conformers were briefly minimized, and the final coordinates were saved into a database. The FlexX module in Sybyl 6.9 was used to dock HBC into the active pocket of C-terminal Ca^{2+}/CaM domain. The NMR structure of the Ca^{2+}/CaM:W7 complex (PDB entry: 1MUX) was retrieved from the Protein Data Bank (PDB). The active site was defined as all the amino acid residues enclosed within a 4.6 Å radius sphere centered by the bound ligand, W7. For the docking of the conformer library of HBC into the target active site, the FlexX docking was performed using the default parameters of the FlexX program with main settings of 100 solutions per iteration during the incremental construction algorithm. The final score for FlexX solutions was calculated by the consensus-scoring program CScore implanted in Sybyl 6.9, and was used for database ranking. The top-ranked conformer of HBC complexed with C-terminal Ca^{2+}/CaM domain was selected as the final model shown in Figure 5.

Western Blot Analysis

HCT15 cells were seeded in 6-well plates (10^5 cells/well), and various concentrations of HBC were treated for the indicated time points. The cell lysates were separated by 10% SDS-PAGE, followed by transfer to PVDF membranes (Milipore, Bedford, MA) using standard electroblotting procedures [46]. Blots were then blocked and immunolabeled overnight at 4°C with primary antibodies, including anti-$p21^{WAF1}$ (Santa Cruz Biotechnology, Santa Cruz, CA), anti-phosphoERK1/2 (Cell Signaling Technology, Inc., Beverly, MA), anti-ERK1/2 (Cell Signaling Technology, Inc.), and anti-tubulin (Upstate Biotechnology, Lake Placid, NY) antibodies. Immunolabeling was detected by an enhanced chemiluminescence (ECL) kit (Amersham Life Science, Inc. Buckinghamshire, UK) according to the manufacturer's instructions.

Cell Cycle Analysis by Flow Cytometry

HCT15 cells were seeded in 6-well plates (10^5 cells/well) and incubated for 24 hr. The cells were starved for 24 hr with serum-free DMEM. After synchronization, the cells were treated with or without HBC, and the incubation was continued for 24 hr in the presence of 10% serum. Then, the cells were harvested with trypsinization, fixed, and permeabilized in the presence of 70% ethanol. The cells were centrifuged and resuspended in phosphate-buffered saline (PBS [pH 7.4]). To reduce background staining, RNase (80 μg/ml) was added, followed by specific DNA-staining using propidium iodide (50 μg/ml). The DNA histograms were determined using a Becton-Dickinson FACS Vantage flow cytometer system (Becton-Dickinson, San Jose, CA), and the cell cycle distribution was analyzed using Cell Quest software version 3.2 (Becton-Dickinson).

Statistical Analysis

Results are expressed as the mean ± standard error (SE). Student's t test was used to determine statistical significance between control and test groups. A p value of <0.05 was considered statistically significant.

Acknowledgments

We are grateful to Dr. J.K. Chen for his critical reading of the manuscript and Dr. J. Yu for his kind help in phage display biopanning. This work was supported by a Molecular and Cellular BioDiscovery Research Program (M1-0311-00-0154) grant from the Ministry of Science and Technology, Republic of Korea, and the Brain Korea 21 Project.

Received: May 23, 2004
Revised: July 22, 2004
Accepted: August 10, 2004
Published: October 15, 2004

References

1. Schreiber, S.L. (1998). Chemical genetics resulting from a passion for synthetic organic chemistry. Bioorg. Med. Chem. *6*, 1127–1152.
2. Harding, M.W., Galat, A., Uehling, D.E., and Schreiber, S.L. (1989). A receptor for the immunosuppressant FK506 is a cis-trans peptidyl-prolyl isomerase. Nature *341*, 758–760.
3. Sche, P.P., McKenzie, K.M., White, J.D., and Austin, D.J. (1999). Display cloning: functional identification of natural product receptors using cDNA-phage display. Chem. Biol. *6*, 707–716.
4. Brown, E.J., Albers, M.W., Shin, T.B., Ichikawa, K., Keith, C.T., Lane, W.S., and Schreiber, S.L. (1994). A mammalian protein targeted by G1-arresting rapamycin-receptor complex. Nature *369*, 756–758.
5. Taunton, J., Hassig, C.A., and Schreiber, S.L. (1996). A mammalian histone deacetylase related to the yeast transcriptional regulator Rpd3p. Science *272*, 408–411.
6. Sharma, S.V., Agatsuma, T., and Nakano, H. (1998). Targeting of the protein chaperone, HSP90, by the transformation suppressing agent, radicicol. Oncogene *16*, 2639–2645.
7. Sin, N., Meng, L., Wang, M.Q., Wen, J.J., Bornmann, W.G., and Crews, C.M. (1997). The anti-angiogenic agent fumagillin covalently binds and inhibits the methionine aminopeptidase, MetAP-2. Proc. Natl. Acad. Sci. USA *94*, 6099–6103.
8. Rodi, D.J., Janes, R.W., Sanganee, H.J., Holton, R.A., Wallace,

B.A., and Makowski, L. (1999). Screening of a library of phage-displayed peptides identifies human bcl-2 as a taxol-binding protein. J. Mol. Biol. *285*, 197–203.

9. Shim, J.S., Kim, D.H., Jung, H.J., Kim, J.H., Lim, D., Lee, S.K., Kim, K.W., Ahn, J.W., Yoo, J.S., Rho, J.R., et al. (2002). Hydrazinocurcumin, a novel synthetic curcumin derivative, is a potent inhibitor of endothelial cell proliferation. Bioorg. Med. Chem. *10*, 2987–2992.
10. Shim, J.S., Kim, J.H., Cho, H.Y., Yum, Y.N., Kim, S.H., Park, H.J., Shim, B.S., Choi, S.H., and Kwon, H.J. (2003). Irreversible inhibition of CD13/aminopeptidase N by the antiangiogenic agent curcumin. Chem. Biol. *10*, 695–704.
11. Burdine, L., and Kodadek, T. (2004). Target identification in chemical genetics: the (often) missing link. Chem. Biol. *11*, 593–597.
12. Cheung, W.Y. (1980). Calmodulin plays a pivotal role in cellular regulation. Science *207*, 19–27.
13. Veigl, M.L., Vanaman, T.C., and Sedwick, W.D. (1984). Calcium and calmodulin in cell growth and transformation. Biochim. Biophys. Acta *738*, 21–48.
14. Kim, D.S., and Suh, K.H. (2001). Cell cycle-dependent activity change of Ca^{2+}/calmodulin-dependent protein kinase II in NIH 3T3 cells. J. Biochem. Mol. Biol. *34*, 212–218.
15. Walsh, M.P., Vallet, B., Autric, F., and Demaille, J.G. (1979). Purification and characterization of bovine cardiac calmodulin-dependent myosin light chain kinase. J. Biol. Chem. *254*, 12136–12144.
16. Colbran, R.J., and Soderling, T.R. (1990). Calcium/calmodulin-dependent protein kinase II. Curr. Top. Cell. Regul. *31*, 181–221.
17. Rybalkin, S.D., and Bornfeldt, K.E. (1999). Cyclic nucleotide phosphodiesterases and human arterial smooth muscle cell proliferation. Thromb. Haemost. *82*, 424–434.
18. Klee, C.B. (1991). Concerted regulation of protein phosphorylation and dephosphorylation by calmodulin. Neurochem. Res. *16*, 1059–1065.
19. Schmidt, H.H., Pollock, J.S., Nakane, M., Forstermann, U., and Murad, F. (1992). Ca^{2+}/calmodulin-regulated nitric oxide synthases. Cell Calcium *13*, 427–434.
20. Wei, J.W., Morris, H.P., and Hickie, R.A. (1982). Positive correlation between calmodulin content and hepatoma growth rates. Cancer Res. *42*, 2571–2574.
21. Schuller, H.M., Correa, E., Orloff, M., and Reznik, G.K. (1990). Successful chemotherapy of experimental neuroendocrine lung tumors in hamsters with an antagonist of Ca2+/calmodulin. Cancer Res. *50*, 1645–1649.
22. Schuller, H.M., Orloff, M., and Reznik, G.K. (1991). Antiproliferative effects of the Ca2+/calmodulin antagonist B859–35 and the Ca(2+)-channel blocker verapamil on human lung cancer cell lines. Carcinogenesis *12*, 2301–2303.
23. Strobl, J.S., and Peterson, V.A. (1992). Tamoxifen-resistant human breast cancer cell growth: inhibition by thioridazine, pimozide and the calmodulin antagonist, W-13. J. Pharmacol. Exp. Ther. *263*, 186–193.
24. Hait, W.N., and Lazo, J.S. (1986). Calmodulin: a potential target for cancer chemotherapeutic agents. J. Clin. Oncol. *4*, 994–1012.
25. Hait, W.N. (1987). Targeting calmodulin for the development of novel cancer chemotherapeutic agents. Anticancer Drug Des. *2*, 139–149.
26. Nakayama, S., and Kretsinger, R.H. (1994). Evolution of the EF-hand family of proteins. Annu. Rev. Biophys. Biomol. Struct. *23*, 473–507.
27. Ikura, M., Clore, G.M., Gronenborn, A.M., Zhu, G., Klee, C.B., and Bax, A. (1992). Solution structure of a calmodulin-target peptide complex by multidimensional NMR. Science *256*, 632–638.
28. Babu, Y.S., Sack, J.S., Greenhough, T.J., Bugg, C.E., Means, A.R., and Cook, W.J. (1985). Three-dimensional structure of calmodulin. Nature *315*, 37–40.
29. Vandonselaar, M., Hickie, R.A., Quail, J.W., and Delbaere, L.T. (1994). Trifluoperazine-induced conformational change in Ca(2+)-calmodulin. Nat. Struct. Biol. *1*, 795–801.
30. Osawa, M., Swindells, M.B., Tanikawa, J., Tanaka, T., Mase, T., Furuya, T., and Ikura, M. (1998). Solution structure of calmodulin-W-7 complex: the basis of diversity in molecular recognition. J. Mol. Biol. *276*, 165–176.
31. Shiotsu, Y., Neckers, L.M., Wortman, I., An, W.G., Schulte, T.W., Soga, S., Murakata, C., Tamaoki, T., and Akinaga, S. (2000). Novel oxime derivatives of radicicol induce erythroid differentiation associated with preferential G(1) phase accumulation against chronic myelogenous leukemia cells through destabilization of Bcr-Abl with Hsp90 complex. Blood *96*, 2284–2291.
32. Bosch, M., Gil, J., Bachs, O., and Agell, N. (1998). Calmodulin inhibitor W13 induces sustained activation of ERK2 and expression of p21(cip1). J. Biol. Chem. *273*, 22145–22150.
33. Villalonga, P., Lopez-Alcala, C., Bosch, M., Chiloeches, A., Rocamora, N., Gil, J., Marais, R., Marshall, C.J., Bachs, O., and Agell, N. (2001). Calmodulin binds to K-Ras, but not to H- or N-Ras, and modulates its downstream signaling. Mol. Cell. Biol. *21*, 7345–7354.
34. Shin, S.Y., Kim, S.Y., Kim, J.H., Min, D.S., Ko, J., Kang, U.G., Kim, Y.S., Kwon, T.K., Han, M.Y., Kim, Y.H., et al. (2001). Induction of early growth response-1 gene expression by calmodulin antagonist trifluoperazine through the activation of Elk-1 in human fibrosarcoma HT1080 cells. J. Biol. Chem. *276*, 7797–7805.
35. Agell, N., Bachs, O., Rocamora, N., and Villalonga, P. (2002). Modulation of the Ras/Raf/MEK/ERK pathway by Ca(2+), and calmodulin. Cell. Signal. *14*, 649–654.
36. Zhang, M., Tanaka, T., and Ikura, M. (1995). Calcium-induced conformational transition revealed by the solution structure of apo calmodulin. Nat. Struct. Biol. *2*, 758–767.
37. Kuboniwa, H., Tjandra, N., Grzesiek, S., Ren, H., Klee, C.B., and Bax, A. (1995). Solution structure of calcium-free calmodulin. Nat. Struct. Biol. *2*, 768–776.
38. Jackson, A.E., and Puett, D. (1986). Binding of trifluoperazine and fluorene-containing compounds to calmodulin and adducts. Biochem. Pharmacol. *35*, 4395–4400.
39. Massom, L., Lee, H., and Jarrett, H.W. (1990). Trifluoperazine binding to porcine brain calmodulin and skeletal muscle troponin C. Biochemistry *29*, 671–681.
40. Hidaka, H., Yamaki, T., Naka, M., Tanaka, T., Hayashi, H., and Kobayashi, R. (1980). Calcium-regulated modulator protein interacting agents inhibit smooth muscle calcium-stimulated protein kinase and ATPase. Mol. Pharmacol. *17*, 66–72.
41. Buday, L., and Downward, J. (1993). Epidermal growth factor regulates $p21^{ras}$ through the formation of a complex of receptor, Grb2 adapter protein, and Sos nucleotide exchange factor. Cell *73*, 611–620.
42. Robinson, M.J., and Cobb, M.H. (1997). Mitogen-activated protein kinase pathways. Curr. Opin. Cell Biol. *9*, 180–186.
43. Pumiglia, K.M., and Decker, S.J. (1997). Cell cycle arrest mediated by the MEK/mitogen-activated protein kinase pathway. Proc. Natl. Acad. Sci. USA *94*, 448–452.
44. Sewing, A., Wiseman, B., Lloyd, A.C., and Land, H. (1997). High-intensity Raf signal causes cell cycle arrest mediated by p21Cip1. Mol. Cell. Biol. *17*, 5588–5597.
45. Neckers, L., and Ivy, S.P. (2003). Heat shock protein 90. Curr. Opin. Oncol. *15*, 419–424.
46. Chae, S.W., Sohn, J.H., Shin, H.S., and Park, Y.E. (2002). Expression of cyclooxygenase-2 protein in gastric carcinogenesis. Cancer Res. Treat. *34*, 252–257.